



3D Stochastic Network Modeling and Investigation of Network Size Effect on the Porous Media Structure of Ion Exchange Catalyst Amberlyst-35 with Computer Programs

Veli SIMSEK^{1*}, Kirali MURTEZAOGLU²

¹ Chemical Engineering Department, Bilecik Seyh Edebali University, 11210, Gulumbe Campus, Bilecik, Türkiye

² Chemical Engineering Department, Gazi University, 06570, Maltepe, Ankara, Türkiye

Highlights

- Fortran77 and Fortran90 programs are used.
- Amberlyst-35 catalyst is simulated.
- GINO is used.

Article Info

Received: 17 Oct 2021
Accepted: 25 July 2022

Keywords

Mercury porosimetry
Amberlyst-35
Stochastic network
mode
Porous media
3D

Abstract

In the present paper, the investigation was focused on the physical characterization and determination of porosity for an ion exchange catalyst called Amberlyst-35, which produces environmentally benign gasoline using 3D network modeling (3DNM). In addition, the effect of the different pore size distributions (PSD) has been investigated in porous media (PM). First, the mercury porosimetry (MPo) experiment was carried out to determine the porosity of the Amberlyst-35. Second, the KALINET program was run by Compact Visual Fortran (CVF) and Graphical Input/Output (GINO) for modeling porous structures. Then, the SECTION program was used for different porous 3D random images. The theoretical penetration curve was drawn using data obtained from the KALINET program and fitted to the experimental penetration values of Amberlyst-35 by changing the number of pores in each pressure interval of the PSD. The PSD was a 3D network model size of (N) = 30x30x30, 40x40x40, 50x50x50, which included 83,700-196,800-382,500 pores, respectively. On the other hand, various sections of the 3D stochastic images of the pore network were obtained from the SECTION program. Finally, 3D network images were drawn by the KALINET3D computer program. The MPo method has been applied using computer programs (with desktop computers). Moreover, it was found that the same results were obtained for both the theoretical and experimental data of MPo.

1. INTRODUCTION

Porous materials (PMA) are natural or artificial solid materials in which the pores in the porous material are heterogeneously or homogeneously distributed in different sizes and shapes [1]. Porous materials are encountered in all areas of life. Influenced by advancing technology, it is becoming increasingly important in nature. Many of the basic materials used in space technology, industry, and daily life are porous [1]. Most of the substances found in nature have a porous structure, albeit a little. Except for artificially produced special cast iron, plastics, and some materials (diamonds, etc.), all of the materials found in nature have different degrees of porosity. If a natural substance or material contains voids in its structure, that material or substance has a porous structure. The gaps in its structure are called pores. Porosity (ϵ) is obtained by the ratio of the total void volume in the material to the total volume of the porous material or material. Porosity is the most essential feature of a porous material. Because porosity and the homogeneous or heterogeneous distribution of pores affect the physical properties of the material [1-3]. For a porous material to have a porous environment, it must have the following properties: a) The material is composed

* Corresponding author, e-mail: veli.simsek@bilecik.edu.tr

of small, interconnected voids that are as small as the material itself. These spaces, which are formed in a solid matrix, contain water, air, or fluid mixtures. b) The fluid should enter from one end of the porous solid material and exit from the other [4].

The pores that create porous environments are often invisible to the naked eye. The reasons why porous materials behave differently from non-porous materials in many cases and the porosity of porous materials are determined by performing a series of tests on the sample and monitoring the behavior of the sample. The interest in understanding the pore structure of porous media has led to the development of pore models in a virtual environment. For this reason, it is important to create pore models and make some predictions on these models to predict the events that may occur in porous structures. Each model reflects the mathematical expression of a hypothesis that deals only with the behavior of certain physical processes. Although the purpose of establishing a model is to answer a specific question, the form of this question is effective in establishing mathematical models [1].

The simulation method (SM) is an increasingly important method in technological developments. And, the simulation consists of a model or models representing a real system. Moreover, computer simulation is also the computer modeling of events based on real data. Due to its success in solving different problems, SM can be used in different fields to achieve different purposes. General-purpose programming languages used in computer languages are FORTRAN, PASCAL, C, and C++. Furthermore, the rapid development of technology has had a positive effect on programming technology. Due to the success of simulation and modeling methods in transforming complex and expensive problems into cheap and straightforward ones, developments in technology have focused on modeling and simulation [1].

The size and shape of the voids found in a natural porous environment are irregular. All the macroscopic properties of PMA are affected by randomness and irregularity. That is, the macroscopic pore structure variables represent the average properties of the porous material. The most important pore structure variables are known as porosity, permeability, and fluid bed. While the fluid bed and porosity represent the properties of the environment, the permeability represents the mass transfer property of the porous medium [5]. Alazmi et al(2000) and Mann et al(1996) stated that the properties of the pores are not only dependent on the size and distribution of the pores, but the most important one is the geometric shapes of the pores [6,7]. It has been determined that the pore environment depends on macroscopic properties such as ejection and suction capillary curves. Permeability and diffusion have been used to form the basis of pore structure models based on microscopic pore structures [8,9]. Fatt(1956) proposed the first network model (NM) composed of regular networks of single-size or varying-size tubes [10]. There are attempts to extract statistical information, such as statistical correlation functions of the pore structure for permeability estimation [11]. In addition to the heuristic methods mentioned, investigators have also used other theories to study PM. The first studies of percolating structures were carried out on random square or cubic lattice structures [12]. After that, 3DNM was obtained using continuum objects placed at random or regular positions [13].

PM is very important in advancing technology [1,5, 14]. Recently, it has been well established by studies. Surface area, pore distribution, and pore volume distribution are important properties of porous materials [1,5,12,15,16]. For example, activated carbon has a high surface area. It is widely used for the removal of chemicals from wastewater. One of the catalyst technologies is used to obtain environmentally benign gasoline. Acidic macro reticular ion-exchange catalysts are commonly used in the production of ethers and to produce environmentally benign gasoline [1, 15], such as Amberlyst-35 [17, 18]. The study was carried out on the Amberlyst-35 catalyst. Amberlyst 35 is a typical macro-reticular resin catalyst that is used in etherification reactions. In the paper, an attempt has been made to understand the effects of pore geometries and network size on the structure of PM in relation to the Amberlyst-35 catalyst sample. The acidic macro reticular resin catalysts are obtained from gel-like micrograins, and macropores are formed from a range of these micrograins that bond to each other at the interface [19]. The $-SO_3H$ groups with strong proton donor-acceptor features act as active regions. These acidic resin catalysts are cross-linked

with polystyrene and divinylbenzene. Macroporous copolymer networks of acidic resin catalysts are composed as a result of the phase separation during the free-radical crosslinking copolymerization of vinyl and divinyl monomers with an inert diluent [19, 20]. According to the International Union of Pure and Applied Chemistry (IUPAC) description, porous materials can be classified into three groups [21]. They are called micropores, mesopores, and macropores. According to the pore width (w), 1. Microporous materials have pore diameters less than 20\AA (Angstrom), 2. Mesoporous materials have pore diameters of 20 to 500, and 3. Macroporous materials have pore diameters larger than 500\AA as well. To better understand the pore structure of catalysts, one has to know how to disperse them. The geometric configuration of the pores in the structure affects the properties of catalysts as well as the pore size opening and distribution [7,8].

The size and shape of the voids in a natural PM are irregular. All the macroscopic properties of PM are affected by randomness and disorder. So, the macroscopic variables of the pore structure represent the average of the porous material. The most important variables in pore structure are porosity, permeability, and flow bed. Streambed and porosity represent features of the medium, and permeability represents the transition feature of the mass of PM [6]. Data from properties such as relative permeability and permeability can be used to make determinations about capillary pressure in pore media [22, 23]. Models of the network were concluded to be a useful method for the behavior of pore size. Network models were represented as physical, so quantitative and expected results were obtained [23]. For this purpose, a 3D stochastic model was developed to simulate porosity, morphology and to research the network size effect on the structure of PM of the Amberlyst-35 catalyst with experimental PMo penetration curves of Amberlyst-35. Its 3D stochastic model was obtained with a CVF compiler and with GINO (Graphical Input/Output). GINO can run them off of subroutine libraries accessible (DIAVOL and CORDNAT) from Fortran (such as Fortran 77, 90, etc.) [24].

2. MATERIALS AND METHOD

In this study, first the KALINET, SECTION, and KALINET 3D programs (the KALINET program works under the CVF compiler for modeling porous materials, the SECTION program is used for different sections of three-dimensional random pore mesh images, and the KALINET3D program is used for 3D mesh drawings) were converted from Fortran77 to Fortran90. This enables commercially supported programs to run under the CVF compiler and with GINO. In the second stage, the parameters obtained as a result of the PMo experiment conducted to determine the porosity of the Amberlyst-35 catalyst used as a catalyst in the production of quality gasoline were modeled in a computer environment. Then, pressure and dimensionless volume values and mercury penetration curves were drawn using the experimental data obtained by PMo, which gives pore volume distribution with the KALINET program. The theoretical penetration curves were created with the obtained pressure and dimensionless volume values. Then, the mercury penetration curve was overlaid with the penetration curves obtained. The pore volume distribution of three-dimensional mesh models with $30\times 30\times 30$ - $40\times 40\times 40$ - $50\times 50\times 50$ sizes and containing 83,700–196,800–382,500 pores was determined, and the effect of mesh sizes on porous materials was investigated. Pore models [25,26] and 3D-size models are given in the appendix [27].

2.1. Transformation on Computer Programs

The KALINET, SECTION, and KALINET 3D programs run under the Compact Visual Fortran compiler: Significant changes were made when converting from Fortran 77 to Fortran 90. Due to some fundamental differences between Fortran90 and Fortran77, some changes have also been made to routines and sub-programs that operate dependently and independently of the main program. The main differences that distinguish Fortran90 from Fortran77 are: dynamically allocating directories by Fortran90; additionally, Case, Exit, Cycle, and Select tags; free format; line skipping; character number, and descriptions written differently. It can be explained by features such as. An example of transformations is given in Tables 1-4 (and the data file is given in the appendix).

Table 1. Conversion from Fortran77 to Fortran90 (KALINET)

Fortran77	Fortran 90
IF(ISGR.EQ.1) THEN NI=2*N+1 NT=3*(N+1)*N**2	IF(ISGR.EQ.1) THEN NI=2*N+1 NT=3*(N+1)*N**2
OPEN(20,FILE='D:\z_Veli\veriler4\Kalineta.out.txt') WRITE(20,110) N,N,N,NT 110 FORMAT(1H1,/,1H0,/,30X,'NETWORK SIZE ',I2,' X ',I2,' X ',I2, \$ /,1H0,/,30X,'NON-SEGREGATED MODEL',/, \$ 30X,'*****',/,1H0,/, \$ 20X,'AND CONTAINING ',I6,' PORES',/,1H0)	OPEN(20,FILE='D:\z_Veli\veriler4\Kalineta.out.txt') WRITE(20,110) N,N,N,NT 110 FORMAT(1H1,/,1H0,/,30X,"NETWORK SIZE ",I2,"X",I2,"X",I2,/,& 1H0,/,30X,'NON-SEGREGATED MODEL',/,& 30X,'*****',/,1H0,/,& 20X,'AND CONTAINING ',I6,' PORES',/,1H0)

In KALINET, the main program was used to create the data file. In the main program and sub-programs, "use gino f90" was written instead of "use gino f77". It is given in Table 2.

Table 2. Conversion from Fortran77 to Fortran90 (SECTION)

Fortran77	Fortran 90
SUBROUTINE SECTON1(N,PL,JPL) C REAL M(61,61,61),PPRE(61,61,61) COMMON /BLK2/FACTOR COMMON /BLK8/M COMMON /BLK11/DDRAW COMMON /BLK22/PPRE	SUBROUTINE SECTON1(N,PL,JPL) ! use gino_F90 use graf_F90 REAL M(101,101,101),PPRE(101,101,101) COMMON /BLK2/FACTOR COMMON /BLK8/M COMMON /BLK11/DDRAW COMMON /BLK22/PPRE

In the SECTION program used for drawing porous structures, conversions were made from Fortran77 to Fortran90. After these processes were carried out, the images of the drawn pores on BMP were formed as dots of the same size. To eliminate these problems, "Call gDrawArcBy2D (0.0, R, 0.0, 0.0, GCLOCKWISE)" was written instead of "CALL gMoveTo2D (X, ZR)" and "CALL DOT (R)" in the KALINET main program. The processes were repeated and the drawings of the pores were made. It is shown in Table 3.

Table 3. Conversion from Fortran77 to Fortran90 (KALINET 3D)

Fortran77	Fortran90
call lincol(1) CALL PORESEC(I,JPL,K) CALL MOVTO2(X,Z) CALL DOT(R) ENDIF 200 CONTINUE	call gSetLineColour(1) CALL PORESEC(I,JPL,K) CALL gMoveTo2D(X,Z) CALL gMoveTo2D(X,Z-R) CallgDrawArcBy2D(0.0,R,0.0,0.0,GCLOCKWISE) ENDIF 200 CONTINUE

In the KALINET 3D program, which is used to draw three-dimensional (3-D) mesh images of pores, in the main program and sub-programs; Use gino_f90 and use graf_F90 were added instead of use gino_f77. It is given in Table 4.

Table 4. Conversion from Fortran77 to Fortran90(SUBROUTINE)

Fortran77	Fortran 90
SUBROUTINE STORE(NI)	SUBROUTINE STORE(NI)
C	!
REAL M(61,61,61),PPRE(61,61,61)	use gino_F90
COMMON /BLK2/M	use graf_F90
COMMON /BLK5/PL	
COMMON /BLK22/PPRE	REAL M(61,61,61),PPRE(61,61,61)
	COMMON /BLK2/M
	COMMON /BLK5/PL
	COMMON /BLK22/PPRE

2.2. Mercury Porosimetry

MPo is one of the methods widely used to determine the pore size distribution of porous materials. The principle of the MPo technique is based on the capillary rise phenomenon, in which mercury behaves as a non-wetting liquid to climb up narrow capillaries. Mercury, unlike most other liquids, has a contact angle (θ) greater than 90° with most solid surfaces. It will not invade a pore or a small orifice unless it is forced to do so by applying suitable pressure. The pressure needed to force the mercury into a circular cylindrical pore can be calculated using the Washburn Equation (1) by assuming that the pore is circular in cross-section and is cylindrical in nature media [1, 28].

$$P = - \frac{2\sigma \cos\theta}{r} \quad (1)$$

P: The applied pressure, N/m²

r: The pore radius

σ : The surface tension of mercury, 480 mN/m²

θ : The contact angle of mercury, 160°

D: The diameter of pore

The data is obtained by PMo essential source for pore geometry. These data are shown graphically in two ways (Figure 1) [1].

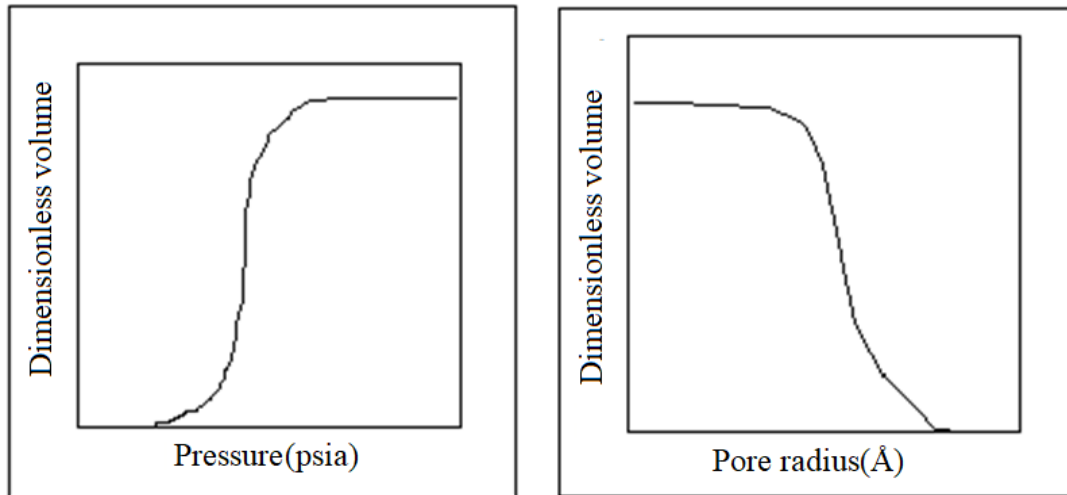


Figure 1. The dimensionless volume with pressure and diameter penetration curves

In this work, the experimental data and the mercury penetration curve are shown in Figure 2. The dimensionless (V/V_{total}) corresponds to a pressure. A pore volume distribution function ($F_v(D)$) is shown Equations (2) and (3) [1] (by using the Washburn Equation and mercury penetration curves (Figure 2))

$$F_v(D) = - \frac{dV}{dD} \quad (2)$$

$$F_v(D) = \frac{\Delta V}{\Delta D} \quad (3)$$

Assuming $V = 0.1$ and calculating the value of ΔD from the mercury penetration curve; a graph D against $F_v(D)$ can be drawn, which gives the pore volume distribution histogram where each histogram bar represents 10% of the pore volume in each pressure range [1].

In this study, the porosity media of a commercial catalyst, Amberlyst-35 (Sigma-Aldrich), was modeled. The properties of Amberlyst-35 were shown in Table 5. Amberlyst-35 was dried overnight at 90°C to remove water from the PM before the mercury experiment was carried out. Apparent pore volume distribution and porosity values of Amberlyst-35 were obtained by PMo, which was conducted with Quantachrome Corporation (Poremaster 60). PMo experiments were conducted on Amberlyst-35 by changing the pressure (6,491-35,410 psia). The contact angle assumed in this work was 160° . The pore volume distribution function, $F_v(D)$, is estimated over several equal volume ranges using the mercury analysis results and the Washburn Equation. In this study, it was taken as $\Delta V = 0.1$. The distribution obtained was converted into a histogram where each histogram block represents 10% of the pore volume. Values are plotted in Table 6 (a, b) and Figure 3. A model has been developed to simulate the porosity and physical characterization of the catalyst: The experimental data were analyzed using a program-solved model, and the proposed model's compatibility with ion exchange catalysts was tested. To carry out a theoretical investigation of the Amberlyst-35 mercury penetration process, the computer programs were evaluated using known random number distribution functions for the pore sizes in a 3-D regular cubic network. All the experiments can be carried out for each of the $N = 30 \times 30 \times 30$, $40 \times 40 \times 40$, $50 \times 50 \times 50$. An application of a 3D network model to mercury porosimetry is given in the appendix [29].

Table 5. Properties of Amberlyst-35[30]

Physical form	Opaque beads
Ionic form as shipped	Hydrogen
Water content	≤3%(H ⁺ form)
Concentration of acid sites	≥5.0 eq(equal)/kg
Average pore diameter	300 Å(Angstrom)
Total pore volume	0.35cc(cm ³)/g
Surface area	50 m ² /g
Maximum operating temperature	150°C

The 3D random network model consists of a cubic network made up of N intersecting cylindrical pore segments in each direction. The diameters of cylindrical pore segments are distributed randomly over the network. The total number of pore segments (N_T) in the entire network is calculated according to the below Equation (4) [1, 28, 31]

$$N_T = 3 * N^2 * (N + 1) \quad (4)$$

where

N: pore segment

(N_T): Total pore segments

The porosity (ϵ) is given by Equations (4) and (5)

$$\epsilon = \frac{\text{Total pore volume}}{\text{Pattern volume}} \longrightarrow \epsilon = \frac{(\pi/4) \sum_{I=1}^{N_T} [RO(I)]^2 * PL}{[PL * (N+1)]^3} \quad (5)$$

where

RO(I): Random pore diameters

N: Network size

N_T : Total number of pores in the regular or irregular cubic network

PL: Pore length

Rearranging

$$PL = \left(\frac{\pi \sum_{I=1}^{N_T} [RO(I)]^2}{4 * \theta * (N+1)^3} \right)^{1/2} \quad (6)$$

Porosity and network size were obtained by using the above Equations (5) and (6). The program generates a set of pore diameters according to a specific version of the model, the four possibilities of which are segregated or non-segregated, fitting or illustration.

Having determined the pore lengths, the pore diameters can be allocated to one of the following assumptions:

- a- Diameters of pores are independent of their lengths.
- b- Diameters of pores may be correlated to their lengths, such as long pores having large diameters and vice versa.
- c- Diameters of pores may be inversely correlated to their lengths, such as long pores have small diameters and vice versa [1, 28, 31]. The penetration program for 3D networks is given in the appendix.

The KALINET program is used as an illustration or fitting method by the International Mathematics and Statistical Libraries (IMSL) or CVF program to generate pore diameters. A theoretical penetration of the network carries it out. Then, total pore volume and data are obtained by the KALINET program and stored in the data file DIAVOL. If the irregular cubic network option is chosen, then the parameters are stored in another data file called CORDNAT. These data files can be read by SECTION and the KALINET3D programs, which are modified to draw mercury penetration steps, based on suitable pressure increments, into a 3D network (Figure 2(a, b)). The program was run to create data files to draw a portion of the overall network size ($N=23$, $NSUB=15$) [28, 32, 33].

The DIAVOL (regular cubic network) or CORDNAT (initial cubic network) file, a whole network of two types can be examined visually, such as:

- a-Sectioning a regular cubic network.
 - b-Cutting an irregular cubic network into sections.
- In the first category, the network is absolutely cubic and can be sectioned in any number of ways.
- 1-Only a horizontal plane cuts the vertical pores (between nodes).
 - 2-Only a horizontal plane cuts vertical and horizontal pores in the plane of the.
 - 3-A plane inclined 45° to the horizontal and the resulting sections may be added randomly displaced and, furthermore, randomly allocated intersection and rotation angles. The nodes can be displaced by a random factor FM (fraction movement) of between 0-0, depending on their original position [1].

In the second category, the network is irregularly cubic and sectioned by an arbitrary plane of the Equation $AX+BY+CZ=D$. The KALINET 3D program can be further utilized for drawing mercury penetration steps into a 3D network by using the data file DIAVOL generated by the KALINET program. The SECTION and KALINET3D programs make use of a drawing library subroutine known as GINO [1].

2.4. Simulation of Amberlyst-35 Catalyst

The apparent pore volume distribution and porosity values for Amberlyst-35 were carried out by the MPo technique. Ring-shaped pellets of catalyst characterization were used to simulate the structures of the wide network that contains millions of pores. Because ring-shaped pellets models are the most widely used 3D pore models for almost all transport events in porous media [1]. Furthermore, random 3D networks were generated by the developed structure of the wide network. Quantitative microscopy and image analysis methods with PMo independent experimental techniques were used. To measure pore structure from 3D random networks, simulation and experimental techniques obtained results comparable to emerging [1]. First, the PMo analysis of Amberlyst-35 was carried out. Following that, the KALINET program, which was run by CVF for modeling of porous structures, The theoretical penetration curve was drawn using data obtained from the KALINET program and fitted to the experimental penetration values of Amberlyst-35 by changing the number of pores in each pressure interval of the PSD. Moreover, various sections of the 3D stochastic pore network were obtained from the SECTION program.

Finally, the MPo method that determines the porosity of the ion exchange catalyst Amberlyst-35 came true with the computer programs. It obtained the same value for both the sectioned image and the experimental

PMo. For experimental data and stochastic network models, computer programs were used, which were executed on a personal computer (desktop computer).

3. RESULTS AND DISCUSSION

A PMo technique has been applied to Amberlyst-35 to obtain an ‘apparent’ pore volume distribution and porosity. The results of PMo experiments were obtained for the Amberlyst-35. PMo experiments conducted with Amberlyst-35 revealed a porosity value of 0.30. It was also observed from the experiments that penetration had begun at different pressures. The penetration interval with Amberlyst-35 has occurred between 64.91-35,410 psia. Penetration had reached 100% at the exit pressure of 35,410 psia for Amberlyst-35. Experimental penetration curves were obtained for Amberlyst-35 catalysts. Experimental and theoretical penetration curves were compared for ion exchange catalysts and are shown in Figure 2. And the theoretical pore volume distribution data of Amberlyst-35 was shown in Tables 6 and 7, respectively. Figure 3(a, b) depicts the theoretical and experimental pore volume distribution of Amberlyst-35.

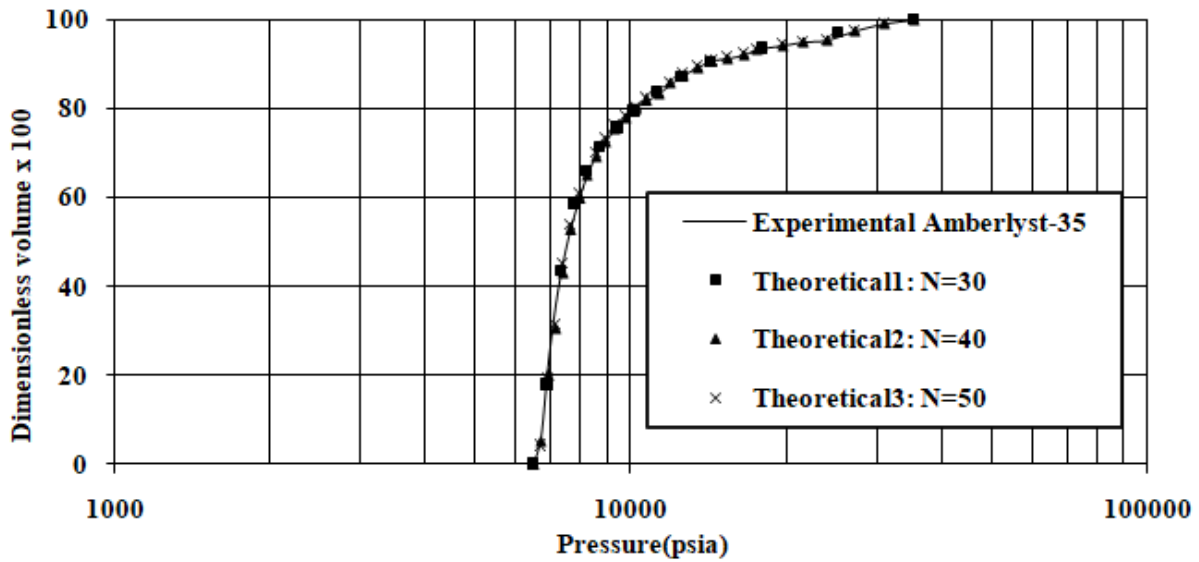


Figure 2. Experimental and theoretical penetration curves of different network size of Amberlyst -35 [1, 34]

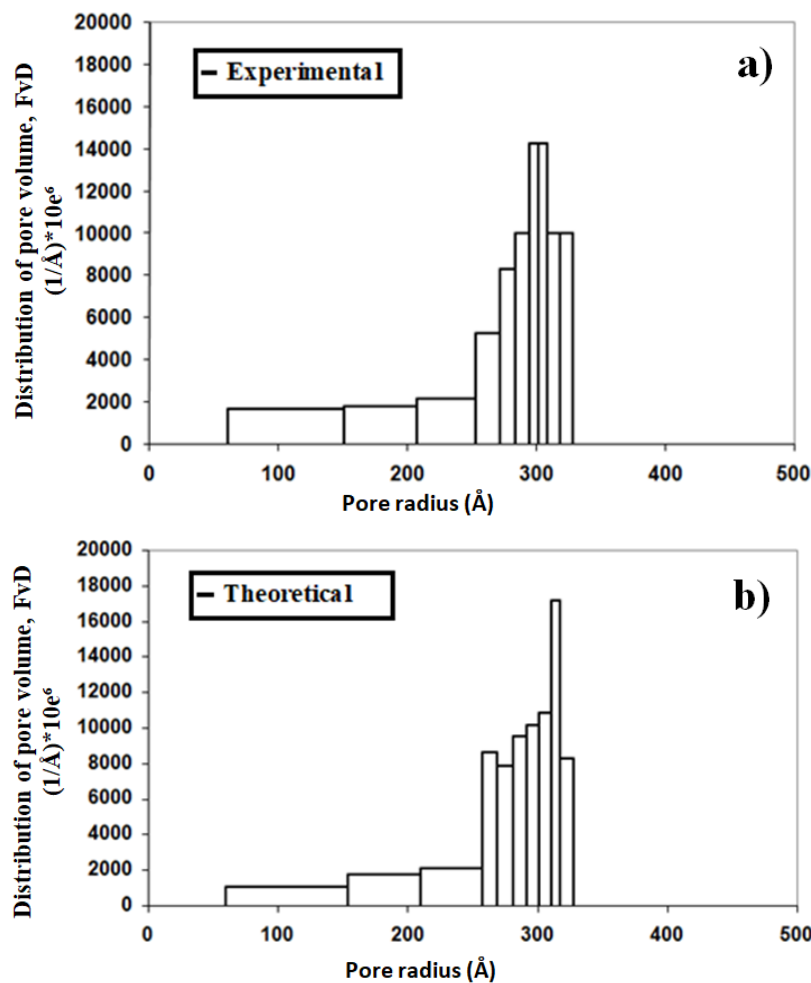
Table 6. The Experimental pore volume distribution data of Amberlyst-35

V=V+dV	*D=D-dD	(dV/dD)x10 ⁶ Å ⁻¹
0.0-0.1	328.60 - 316.50	9999
0.1-0.2	316.50 - 310.69	9999
0.2-0.3	310.69 - 301.51	14285
0.3-0.4	301.51 - 291.70	14285
0.4-0.5	291.70 - 281.20	9999
0.5-0.6	281.20 - 268.53	8332
0.6-0.7	268.53 - 256.95	5262
0.7-0.8	256.95 - 209.91	2172
0.8-0.9	209.91 - 154.15	1786
0.9-1.0	154.15 - 60.2	1659

*D= Pore diameter

Table 7. The Theoretical pore volume distribution data of Amberlyst -35

$V=V+dV$	$*D=D-dD$	$(dV/dD) \times 10^6 \text{ \AA}^{-1}$
0.0-0.1	328.60 - 316.50	8264
0.1-0.2	316.50 - 310.69	17212
0.2-0.3	310.69 - 301.51	10893
0.3-0.4	301.51 - 291.70	10194
0.4-0.5	291.70 - 281.20	9524
0.5-0.6	281.20 - 268.53	7893
0.6-0.7	268.53 - 256.95	8636
0.7-0.8	256.95 - 209.91	2126
0.8-0.9	209.91 - 154.15	1793
0.9-1.0	154.15 - 60.20	1064

**Figure 3.** Distribution of pore volume experimental(a) and theoretical(b) of Amberlyst-35

In the second part of the proposed model; parameters were obtained to be used in a computer program by evaluation of MPo experiments conducted with ion-exchange resins. A theoretical model was solved by KALINET, a model that used Compact Visual Fortran90. The model's theoretical penetration curves were fitted to experimental values by changing the number of curves in each pressure interval (Figure 2). In addition, the effect of different pore sizes was investigated in PM (Figure 3). The pore size distribution was done by the $N = 30 \times 30 \times 30 - 40 \times 40 \times 40 - 50 \times 50 \times 50$ 3D network model size, which included 83,700-196,800-

382,500 pores. Vertical cross-sections of Amberlyst-35 are shown in Figure 4 (a, b), and (c), respectively. Smooth and rough ellipse pores of Amberlyst-35 are shown in Figure 5 (a, b), and (c), respectively.

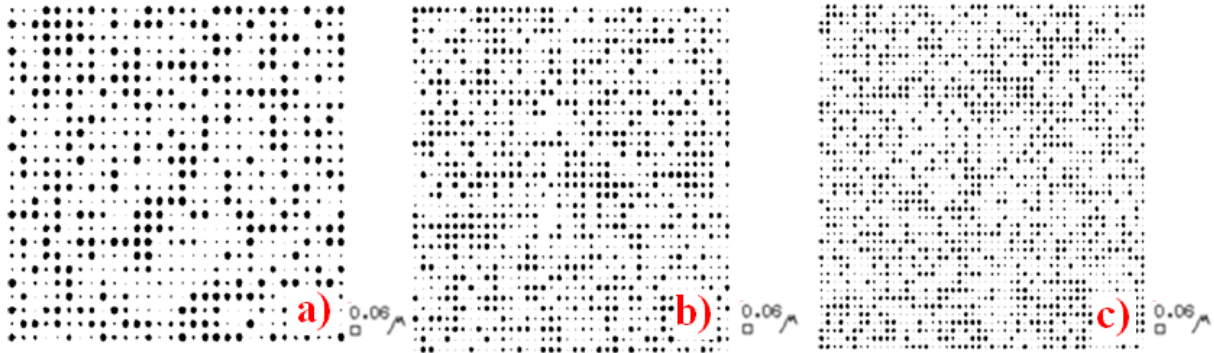


Figure 4. Vertical cross section of porous Amberlyst-35 catalysts with dimensions a) $N=30 \times 30 \times 30$, b) $N=40 \times 40 \times 40$, c) $N=50 \times 50 \times 50$ diameters: $D_{min} - D_{max} = 60.2 - 328.6 \text{ \AA}$, pressure interval 35410-6491psia)

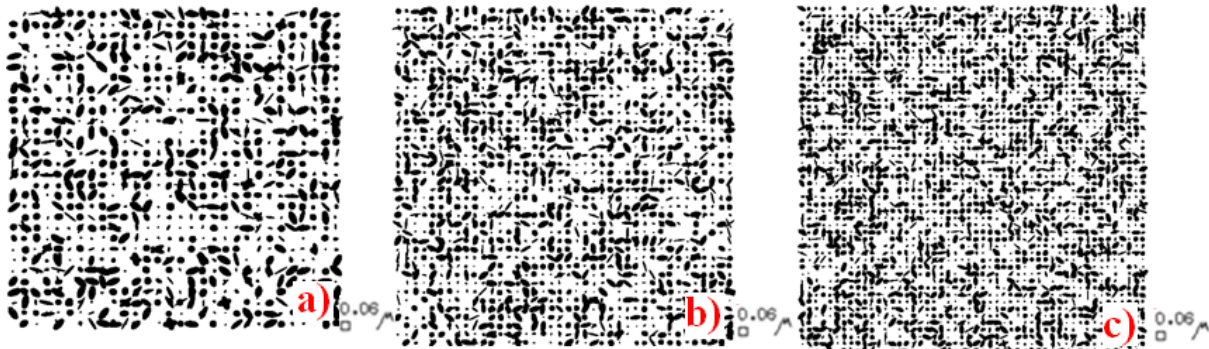


Figure 5. Smooth and rough ellipse porous of Amberlyst-35 catalysts with dimensions; a) $N=30 \times 30 \times 30$, b) $N=40 \times 40 \times 40$, c) $N=50 \times 50 \times 50$ diameters: $D_{min} - D_{max} = 60.2 - 328.6 \text{ \AA}$, pressure interval 35,410-6,491psia)

If a regular cubic model is needed, then pore length (PL) is allocated as length to each of the pores and the diameters are allocated to the pores. On the other hand, if an irregular cubic is required, then the network is initially assumed to be cubic with pores of the same equal length PL. Figure 6 (a, b) depicts regular and irregular cubic network samples. Moreover, an ellipse can also be drawn with a winding/rotating axis, such as a rough circumference. It is done by randomly dividing the horizontal into 3 segments and rotating the two end segments by a limited random angle (Figure 7). Figure 7 shows an example of a three-dimensional (3D) section of the rough and tortuous/rotating) ellipse. The data file is given in appendix (data files for the SECTION program N: 30X30X30).

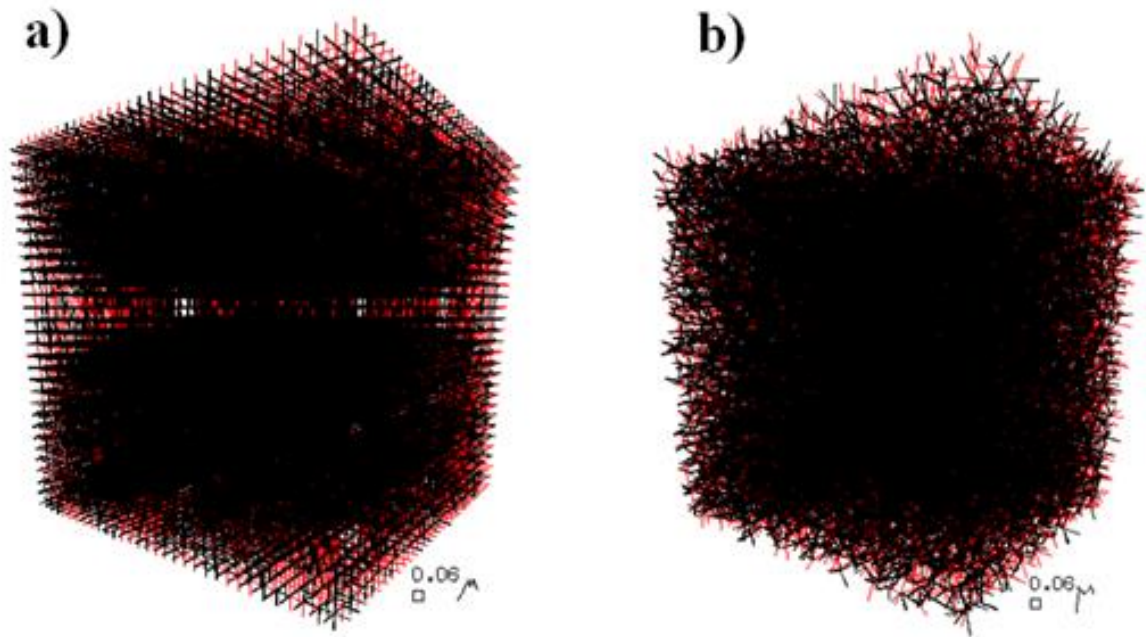


Figure 6. a) Regular network model, $D_{min}=60.2\text{\AA} - D_{max}=328.6\text{\AA}$, (35,410-6,491psia, $N=30$), b) Irregular network model, $D_{min}=60.2\text{\AA} - D_{max}=328.6\text{\AA}$, (35,410-6,491psia, $N=30$)

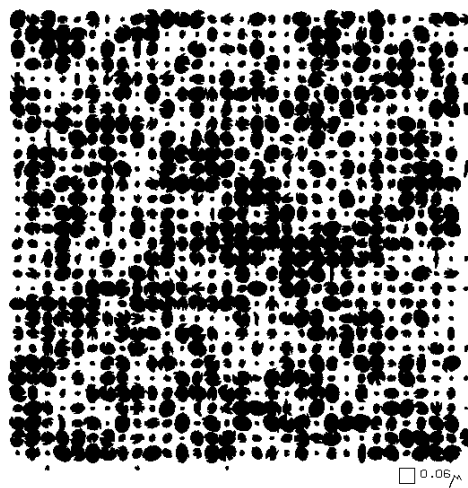


Figure 7. An example of a three-dimensional (3-D) section of the rough and tortuous/rotating ellipse (IELIPSE=3, 6491-35410psia, $328.6 - 60.2\text{\AA}$)

3D drawings with different pore diameters ($N = 30 \times 30 \times 30$) applications obtained from the SECTION program (Figure 8). The data file is given in appendix (data files for the SECTION program N:30X30X30).

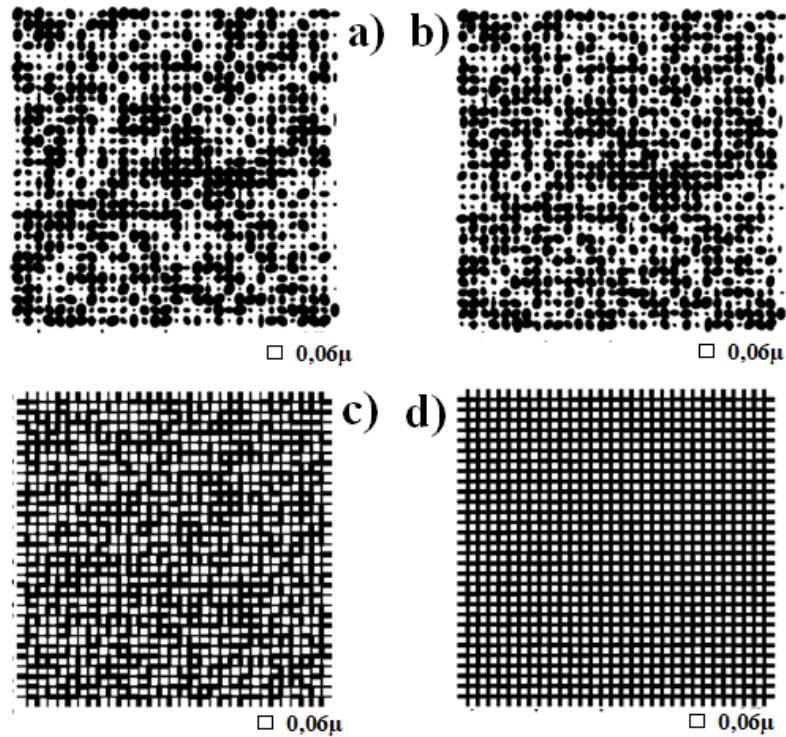


Figure 8. a) ISECT5(IELIPSE2) $D_{min-max}=60.2-328.6 \text{ \AA}$ (35410-6491 psia), b) ISECT5(ELIPSE2) $D_{min-max}=100-328.6 \text{ \AA}$ (21330 - 6491 psia), c) ISECT 2; $D_{min-max}= 100-328.6 \text{ \AA}$ (21330 - 6491 psia), d) ISECT 2; $D_{min-max}= 280-328.6 \text{ \AA}$ (7618 – 6491 psia)

It is seen from the Figures that the porosimetry results obtained with the model were fitted with experimental results. In the next step, sections of the images of the 3D stochastic pore network were obtained from the program SECTION for each network size, which used the data generated by KALINET. 3D network images of porous media were drawn by the KALINET 3D computer program using the data from the KALINET program (the data file is given in the appendix: data file and computer output from the KALINET program for Figure 6). The visual penetration of mercury in the network can be observed with the help of these 3D network drawings for different pressure intervals. Figure 9 (a, b, c, d) shows a 3D different network size model of Amberlyst-35.

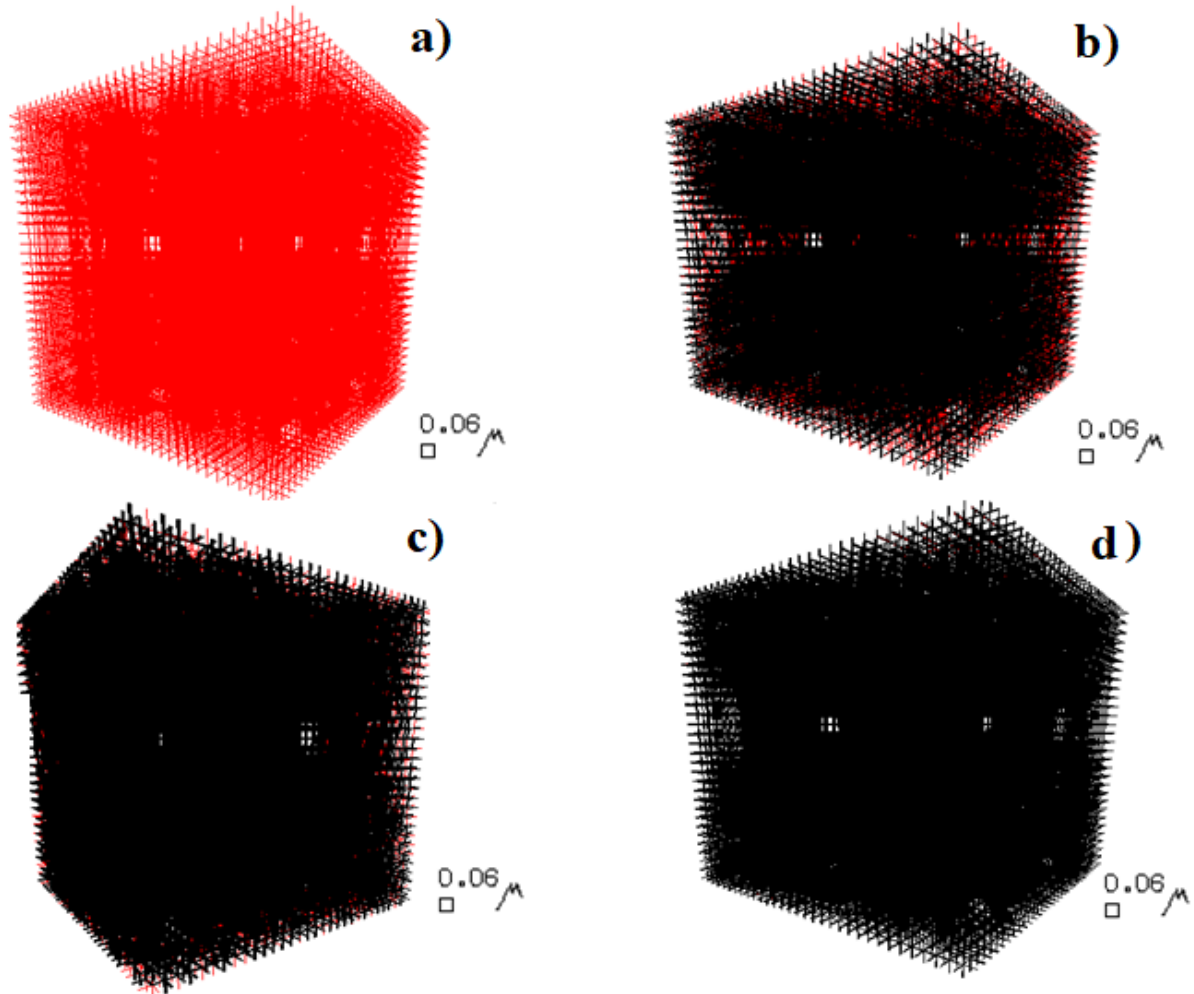


Figure 9. 3D different network size ($N=30 \times 30 \times 30$) models for different pressure intervals of Amberlyst-35, a) $D_{min}=902 \text{ \AA}$, 1,940.12 psia, b) $D_{min}=200 \text{ \AA}$, 10664.7 psia, c) $D_{min}=100 \text{ \AA}$, 26,119.25 psia, d) $D_{min}=60.2 \text{ \AA}$, 35,410 psia

4. CONCLUSION

The pore structure of the porous materials is highly complex and randomly created, so the workers in this field of research have made simplified assumptions about interpreting structures, for which no adequate description is yet available. The workers studying in this field have tried to model specific properties of their particular PM by using one experimental method, and in some cases, two or more methods to confirm the results. The computer simulation models that have so far been developed are based on a particular type of experimental method in which prediction of porous media's properties has been achieved successfully.

In this work, experimental and computer simulation techniques have been used to determine the pore size distribution of Amberlyst-35 porous media. The results of these porosimetric investigations have been simulated by running a redeveloped stochastic 3DNM, which can now be executed on a personal computer. Theoretical penetration curves were obtained and fitted to experimental penetration curves by varying the number of pores in each pressure/diameter interval over the 3DNM. The visual penetration of mercury in the network can be observed with the help of these 3D network images obtained at different pressure intervals. According to the experimental and theoretical results obtained, this paper shows that the 3DNM is a realistic application to characterize the pore structure of PM relative to mercury penetration into pores.

CONFLICTS OF INTEREST

No conflict of interest was declared by the authors.

REFERENCES

- [1] Simsek, V., "Application of mercury porosimetry to three dimensional(3D) stochastic network model and researching network size effect on structure of porous media", MSc Thesis, Gazi University Graduate School of Natural and Applied Sciences, (2008).
- [2] Huysmans, M., Dassargues, A., "The effect of heterogeneity of diffusion parameters on chloride transport in low-permeability argillites", *Environmental Earth Sciences*, (2012). DOI:10.1007/s12665-012-1871-0
- [3] Dultz, S., Simonyan, A.V., Pastrana, J., Behrens, H., Plötze, M., Rath, T., "Implications of pore space characteristics on diffusive transport in basalts and granites", *Environmental Earth Sciences*, 69: 969–985, (2013). DOI: 10.1007/s12665-012-1981-8
- [4] Ishakoğlu, A., Boytaş, A. F., " Measurement and evaluation of saturations for water, ethanol and light non- aqueous phase liquid in a porous medium by gamma attenuation", *Applied Radiation and Isotopes*, 56: 60-606, (2002).
- [5] Dullien, F.A.L., "Porous media, fluid transport and pore structure", Academic Press San Diego, 1-4, (1992).
- [6] Alazmi, B., Vafai, K., "Analysis of variants within the porous media transport models", *Journal of Heat Transfer*, 122: 303-326, (2000).
- [7] Mann, R., El-Nafaty, U.A., "Probing internal structures of FCC catalysts particles: From parallel bundles to fractals", *Studies in Surface Science and Catalysis*, 100: 355-364, (1996).
- [8] Rieckmann, C., Keil, F.J., "Multicomponent diffusion and reaction in 3-D networks", *Industrial & Engineering Chemistry*, ACS Publications, 3275-3281, (1997).
- [9] Sahimi, M., "Flow and Transport in Porous Media and Fractured Rock: From Classical Methods to Modern Approaches", VCH, Weinheim, Germany, (1995).
- [10] Fatt, I., " The network model of porous media I. Capillary pressure characteristics", *Transactions of the AIME*, 207: 144–159, (1956). DOI: <https://doi.org/10.2118/574-G>
- [11] Feng, X., Yin Y., "Geometry models of porous media based on Voronoi tessellations and their porosity–permeability relations", *Computers & Mathematics with Applications*, 72: 328-348, (2016).
- [12] Kirkpatrick, S., "Percolation and conduction", *Reviews of Modern Physics*, 45(4): 574–588, (1973).
- [13] Balberg I., "Recent developments in continuum percolation", *Philosophical Magazine Part B*, 56(6): 991-1003, (1987).
- [14] Benham, G., Bickle, M., Neufeld, J., "Upscaling multiphase viscous-to-capillary transitions in the heterogeneous porous media", *Journal of Fluid Mechanics*, 911 A59, (2021). DOI:10.1017/jfm.2020.1134

- [15] Dogu, T., Boz, N., Aydın, E., Oktar, N., Murtezaoglu, K., Dogu, G., "Drift Studies for the reaction and adsorption of alcohols and isobutylene on acidic resin catalysts and the mechanism of ETBE and MTBE synthesis", *Industrial & Engineering Chemistry Research*, 40: 5044-51, (2001).
- [16] Simsek, V., Avci, P., "Characterization and catalytic performance of modified sba-16 in liquid phase reaction", *International Journal of Chemical Reactor Engineering*, (2018). DOI: <https://doi.org/10.1515/ijcre-2017-0246>
- [17] Simsek, V., "Investigation of catalytic sustainability of silica-based mesoporous acidic catalysts and ion-exchange resins in methyl acetate synthesis and characterizations of synthesized catalysts", *Arabian Journal for Science and Engineering*, 44: 5301-5310, (2019). DOI: 10.1007/s13369-018-3570-y
- [18] Yang, A., Antrassian C., Kurtzman J., "Production of Dimethyl Ether (DME) for Transportation Fuel", *Senior Design Reports (CBE) University of Pennsylvania Scholarly Commons*, 4(21): 1-190, (2020).
- [19] Dogu, T., Aydın, E., Boz, N., Murtezaoglu, K., Dogu, G., "Diffusion resistances and contribution of surface diffusion in TAME and TAEF production using Amberlyst - 15", *International Journal of Chemical Reactor Engineering*, A6 1-9, (2003).
- [20] Boz, N., Dogu T., Murtezaoglu K., Dogu, G., "Effect of hydrogen ion- Exchange capacity on activity of resin in tert-amyl-ethyl-ether synthesis", *Applied Catalysis a General*, 268: 175-182, (2004).
- [21] IUPAC, "Manual of symbols and terminology", *Pure Applied Chemistry*, 31: 578, (1978).
- [22] Jiang, Z., Van Dijke, M.J., Wu, K., Couples, G.D., Sorbie, K.S., Ma, J., "Stochastic Pore Network Generation from 3D Rock Images", *Transport in Porous Media*, 94: 571-593, (2012). DOI: 10.1007/s11242-011-9792-z
- [23] Matthew, T.B., Karsten, E.T., Hjortso, M., "Coupling pore-scale Networks to continuum scale models of porous media", *Computers & Geosciences*, 33: 393-410, (2007).
- [24] Woodsford, P.A., "The design and implementation of the GINO 3D graphics software package", *Software-Practice and Experience*, 1, 4, (1971).
- [25] Rigby, S.P., Gladden, L. F., "Deconvolving pore shielding effects in mercury porosimetry data using NMR techniques", *Chemical Engineering Science*, 55: 5599-5612, (2000).
- [26] Allamy, A., Mann, R., Holt, A., "Modeling of catalyst particle skin effects using a 3-D pore network model and quantitative microscopy", *Chemical Engineering Science*, 58(10): 1989-2000, (2003).
- [27] Kzenzhik, O. S., "Capillary equilibrium in porous media with intersecting pores", *Zhurnal Fizicheskoi Khimii*, 36: 691, (1963).
- [28] Sbaiti, B., "Modelling of oil bearing rock using a three dimensional network model", MSc. Thesis, University of Manchester Institute of Science and Technology, Manchester, 1-40, (1983).
- [29] Golshan, H., "Development and application of stochastic pore structure models", PhD Thesis, University of Manchester Institute of Science and Technology, Manchester, 1- 75, (1979).
- [30] URL, <https://www.lenntech.com/Data-sheets/Dow-Amberlyst-35-dry-L.pdf>. Accessed Date: 19.04.2021

- [31] Mürtezaoğlu, K., "Further developments in the use of visualised porosimetry for PVC structure characterization", Ph.D. Thesis, University of Manchester Institute of Science and Technology, Manchester, 6-54, 65-104, (1994).
- [32] Khalaf, K.M., "Characterisation of FFC catalyst particles using 3-D stochastic pore networks", Ph.D. Thesis, University of Manchester Institute of Science and Technology, Manchester, 1-100, (1998).
- [33] Roudaki, S.J.M., "Application of three – dimensional stochastic pore network to zinc oxide particles", M.Sc. Dissertation, University of Manchester Institute of Science and Technology, Manchester, 1-40, (1989).
- [34] Simsek, V., Oktar, N., Mürtezaoğlu, K., "Application of mercury porosimetry to three dimensional (3D) stochastic network model on ion exchange resins", 5th Chemical Engineering Conference for Collaborative Research in Eastern Mediterranean Countries -EMCC5 May 24-29, (2008).

APPENDIX

Pore Models:

The pores that create porous environments are often invisible to the naked eye. Therefore, the reasons why porous materials behave differently than non-porous materials in many cases are determined by monitoring the behavior of the sample by performing a series of tests on it. The basis of the modeling performed in this study was formed with real data. In other words, it was taken into consideration that the modeling is compatible with real data, simplifying the complex structure and ultimately reflecting the real situation. Because of these features of modeling (stochastic modeling) with multiple inputs and multiple output possibilities, in which inputs and outputs are random with the trial and error method, prioritizing real characteristics is used.

PSD and pore parts were extracted with MP penetration curves [25]. This data has been adapted using the Deshielding method. The collected data was combined with NMR (Nuclear Magnetic Resonance Spectroscopy), shell density, and shell cage residence time. With the deshielding method, the dispersion phenomenon in the pores has a spatial geometric structure that is not possible with traditional methods [26]. Pore models can be classified in three different ways according to their use:

1. One-dimensional models (such as parallel tube bundle models).
2. Two-dimensional models (such as network models).
3. Three-dimensional models (such as global package models) [26].

3D-size models:

Spherical pack models are the most commonly used three-dimensional pore models for almost all transport phenomena in PM. Developments on these models: 3D-size model is based on the development of "random spherical packet models" in a projected porous material, in which the pore consists of spaces between microspheres, consisting of a large number of randomly overlapping solid microspheres [1]. Studies on three-dimensional pore networks are very old, and in almost all cases, it is predicted that the pores are cylindrical, just like in two-dimensional networks. The most natural network is the one in which the connectivity factor is equal to 10. The model is used to indicate the effect of the pore distribution of the porous medium in porous materials on the penetration of mercury into the pores. The radii of the pores are randomly distributed on the web, predicting that the nodes have zero volume [27].

Table: The commands used in this study with their explanations

FORTRAN 77	FORTRAN 90	EXPLANATION
GINO	gOpenGino	Starts the Gino program

PICBEG	gOpenSeg	Starts the new segment
MOVTO2	gDrawLineTo2D	Determines the position of the points (within 2D with the absolute value)
MOVTO3	gDrawLineTo3D	Determines the position of the points (within 3D with the absolute value)
BROKEN	gSetBrokenLine	Selects line types
BUFLIM	gSetWorkspaceLimit	Determines the workspace area
CHAFIX	gDisplayRealFixed	Follows the actual values of fixed points
CHASTR	gDisplayStr	Character index of outputs
DEBUG	gDebug	Follows the flow of information within Gino
DEVEND	gCloseDevice	Terminate device output
DEVFIL	gSetDeviceFilename	(separation)
DEVSUS	gSuspendDevice	Selects the output file
ERRMAX	gSetMaxErrorLimit	Suspends emerging devices
GINEND	gCloseGino	Determines the maximum error numbers
LINCOL	gSetLineColour	Closes the Gino program
LINBY2	gDrawLineBY2D	Makes the choice of color
LINBY3	gDrawLineBY3D	Draws line segments (in 2D)
MOVBY2	gMoveBy2D	Draws line segments (in 3D)
MOVBY3	gMoveBy3D	Determines the position of the points (within 3D with relative value)
MOVTO2	gMoveTo2D	Determines the position of the points (within 2D with the absolute value)
MOVTO3	gMoveTo3D	Determines the position of the points (within 3D with the absolute value)
PICDRA	gDrawSeg	Redraws the existing line segment
PICEND	gCloseSeg	Closes the currently opened segment
ROTAT2	gRotate2D	X allows Y to rotate around the origin
ROTAT3	gRotate3D	Makes the rotation of X, Y and Z around the origin.
SDFBUF	gDefineSegWorkspace	Creates workspace to view files in software
SHEAR2	gShear2D	Cuts the X and Y axis

SHEAR3	gShear3D	Cuts the X, Y, and Z axes
SHIFT2	gShift2D	Allows X and Y to replace the origin axis
SHIFT3	gShift3D	Allows X, Y and Z to be displaced on the origin axis.
WINDO2	gSetWindow2D	Windows defines u in 2D
WINDO3	gSetWindow3D	Windows definitions in 3D
WINDOW	gSetWindowMode	Used for embedding windows structure
VIEW	gGenerateView	Generate view transformation
ARCBY2	gDrawArcBy2D	Draws the circle with relative value within 2D
BMG	gBmg	Framework (Bitmap)
MWIN	gMwin	Opens default windows
BOX	gDrawBox	Drawing area

Application of a 3D network model to mercury porosimetry:

Computer programs, to carry out a theoretical investigation of the mercury penetration process were developed originally by Golshan [30]. A theoretical investigation of any powder or pellets using known distribution functions for the pore sizes in a 3D regular cubic network was done by Sbaiti [28]. The model was redeveloped by Murtezaoglu [31] and carried out for the characterization of PVC powder. It was run by using numerical algorithms group (NAG) and graphics software package (GINO) programs on the Manchester Computer Centre (MCC) main frame. Moreover, the 3D regular cubic network has been working without the need for a further support center on the main frame [31]. To carry out this theoretical penetration on the network, the following assumptions were needed:

- a-Pore segment length is the same for all segments.
- b-The shape of the pore segment is cylindrical.
- c-The network is a cubic one, and the inter-connectivity factor is constant and equal to 10.
- d-The periphery of the network is in direct contact with the surrounding mercury.
- e- At first, the entire network is completely vacuumed [1, 28, 31].

Penetration program for 3D network:

The KALINET computer program is used to compute the penetration for segregated and nonsegregated models. It is designed to run with a data file whose underlying parameters contain:

1. Type of mode and network.
2. Minimum-maximum diameter, diameter step, porosity, number of simulations, tolerance for porosity.
3. Network size.
4. Number of intervals.
5. Number of pores in each interval.
6. Boundaries of the intervals [1,4].

The KALINET computer program can be run 'illustration' or 'fitting'. The illustration mode is where some standard pore size distribution (such as uniform bimodal or normal, anti-normal, etc.) is used. This mode is used to compare the effects that different distributions have on the penetration curve. The second (fitting) version is essentially when an empirical size distribution is searched out to replicate a penetration curve. This process is performed by assigning a variable number of pore interval boundaries and then assigning different numbers of pores to these intervals in a trial and error procedure (appropriate minimum-maximum pore diameter range) until the theoretical penetration curve coincides with the experimental penetration

curve (Simsek 2008; Ishakoğlu and Boytaş 2002). The data file below contains the mode and network type (2,1,2), minimum-maximum diameter(60.2-328.6), diameter step(10), porosity (0.30), number of simulations (0), porosity tolerance (0.01), network size(30x30x30), number of intervals (1,1), number of pores in each interval, and interval boundaries (2,2,2).

DATA FILE (N = 30x30x30 FOR KALINET PROGRAM)

2 , 1 , 2

0.001

60.2, 328.6 , 60.2, 10.0 , 30 ,0 , 0.30, 0.01

30

11

28900 , 4200 , 4000 , 2250 , 1000 , 1000,

4000, 3550,7300, 9000, 18500

60.2, 85.,107., 124., 134., 144., 151.,

170., 188., 247., 314.4, 328.6

2 , 2 , 2

DATA FILES FOR THE SECTION PROGRAM (30x30x30)

a) for ISECT1 ;

30 , 1 , 1

60.2 , 328.6, 10.0 , 60.2

21

b) for ISECT2 ;

30 , 1 , 2

60.2, 328.60, 10.0 , 60.2

12

c) for ISECT3;

30 , 1 , 3

60.2, 328.60, 10.0 , 60.2

0.1, 1

d)for ISECT4 (ELIPS1) ;

30 , 1 , 4

60.2, 328.6, 10.0 , 60.2

1.0,-2.0,1.0,0.0,1.0

d)for ISECT4 (ELIPS2);

30, 1, 4

60.2, 328.6, 10, 60.2

1.0, -2.0, 1.0, 0.0, 2.0

0.7

d)for ISECT4 (ELIPS3);

30, 1, 4

60.2, 328.6, 10, 60.2

1.0, -2.0, 1.0, 0.0, 3.0

0.7